Supporting Information

Amphiphilic composite material of titanosilicate@mesosilica/carbon as Pickering catalyst

Yu Ding, Hao Xu*, Haihong Wu*, Mingyuan He, and Peng Wu*

Shanghai Key Laboratory of Green Chemistry and Chemical Process, School of Chemistry and Molecular Engineering, East China Normal University, North Zhongshan Rd. 3663, Shanghai 200062, China

E-mail: pwu@chem.ecnu.edu.cn, hhwu@chem.ecnu.edu.cn, hxu@chem.ecnu.edu.cn

Experiment Section

Chemicals and Reagents

All chemicals and reagents were obtained from commercial suppliers and used without further purification: tetraethylorthosilicate (Sigma-Aldrich, 98% Reagent Grade), tetrabutyltitanate (Sigma-Aldrich, 98% Reagent Grade), tetrapropylammonium hydroxide (TCI, 25 wt.% in water), ethanol (Sinopharm Chemical Reagent Co., Ltd., Reagent Grade), ammonia solution (Sinopharm Chemical Reagent Co., Ltd., 28 wt.%), cetyltrimethylammonium chloride (J&K Co.), resorcinol (J&K Co.), formaldehyde solution (Sinopharm Chemical Reagent Co., Ltd., Reagent Grade，37 wt% aqueous solution stabilized with 8-14% methanol).

Material Synthesis

Synthesis of TS-1 titanosilicate

TS-1 was hydrothermally synthesized according to previously reported method.[1] A mixture of tetraethylorthosilicate (TEOS) and tetrabutyltitanate (TBOT) was dropped

into the solution containing water and tetrapropylammonium hydroxide (TPAOH). After hydrolysis under stirring at 313 K for 1 h, a gel was formed. Further removal of ethanol was carried out by heating the gel to 353 K and stirring for 2 hours. Then, the resulting sol-gel with a molar composition of 1.0 SiO_2: 0.025 TBOT: 0.18 TPAOH: 18H_2O was then transferred to a Teflon-lined autoclave at 443 K for 2 days. The product was recovered by centrifugation, washed with deionized water, and dried at 373 K for 12 h. The calcination was carried out at 823 K in air for 6 h to remove the occluded organic species.

Preparation of TS-1@silica/carbon (TS-1@Si/C) hybrid material

The TS-1@Si/C hybrid material was prepared with TS-1 crystal as core and mesoporous silica/carbon as shell. In a typical synthesis, 0.9 g of TS-1 powder was added into the mixture of 97.0 mL of ethanol, 198.9 mL of water and 1.3 mL of ammonium hydroxide solution (28 wt.%), and stirred for 0.5 h, followed by an ultrasonic treatment for 1 h. Then, 1.5 g of cetyltrimethylammonium chloride (CTAC) was added into the mixture under vigorous stirring. Afterwards, 0.31 g of resorcinol (9 mM) was added to the mixture and stirred for 0.5 h. Then, 0.42 mL of formaldehyde solution (37 wt.%) and 1.255 mL TEOS were added simultaneously to form the final mixture, which was stirred at room temperature for 12 h. Various TS-1@Si/C materials were similarly prepared by varying the initial TEOS/resorcinol ratio, but keeping the total concentrations of TEOS and resorcinol constant at 28.0 mM. For all the experiments, the resorcinol/formaldehyde molar ratio was kept at 0.5 and the ethanol/water ratio was 0.5 : 1 (v/v). The obtained mixture was transferred to a Teflon-lined stainless steel autoclave and heated at 373 K for 24 h. After the autoclave was naturally cooled to room temperature, the solid products were collected by washing with deionized water and ethanol, and drying at 323 K overnight. They

were calcined at 823 K in N_2 atmosphere for 6 h to complete the carbonization of resol and allow the decomposition of occluded surfactant template. The obtained composites were denoted as TS-1@Si/C-*x*, where *x* represents the initial TEOS/resorcinol ratio.

Preparation of TS-1@C-D and TS-1@Si-D materials

The core-shell structured materials, with only carbon or silica component in the shell, were prepared under a similar experimental process as that of TS-1@Si/C. The one with only carbon shell was prepared using 28.0 mM resorcinol and 56.0 mM formaldehyde as carbon precursor, while 28.0 mM TEOS was used as silica precursor to synthesize the material with only silica component in the shell. The resultant materials were denoted as TS-1@C-D and TS-1@Si-D, respectively, meaning directly synthesized core-shell structured material with only carbon or silica component in the shell.

Preparation of TS-1@C-R and TS-1@Si-R materials

The core-shell structured materials, with only carbon or silica component in the shell, could also be prepared by selectively removing the silica or carbon species in shell. The silica component could be selectively removed by the treatment in TPAOH aqueous solution, which was supposed to dissolve the silica species in the shell without ruining the TS-1 core crystals. Typically, the TS-1@Si/C composite was stirred in 0.5 M TPAOH solution at 338 K for 4 h with the liquid/solid mass ratio of 200, followed by calcination at 823 K in N_2 atmosphere for 6 h to decompose the TPAOH species, giving rise to the TS-1@C-R material composed of carbon shell and TS-1 core. On the other hand, the carbon component was selectively removed by

calcination at 823 K in air for 6 h, resulting in TS-1@Si-R material.

Preparation of TS-1(0.2)@Si/C-13, TS-1(0.5)@Si/C-13, TS-1(1.2)@Si/C-13 and TS-1(2.0)@Si/C-13 materials

A series of core-shell structured TS-1@Si/C materials, with different shell thickness but the same TEOS/resorcinol ratio of 13, were prepared under a similar experimental process as that of TS-1@Si/C, *via* changing the TS-1 amount (0.2, 0.5, 1.2 and 2.0 g) in the synthetic system. The finally obtained materials with different shell thickness were denoted as TS-1(0.2)@Si/C-13, TS-1(0.5)@Si/C-13, TS-1(1.2)@Si/C-13 and TS-1(2.0)@Si/C-13.

Characterization techniques

The X-ray diffraction (XRD) patterns were taken on a Rigaku Ultima IV diffractometer with Cu-Kα radiation (λ = 1.5405 Å) at 35 kV and 25 mA. The contents of Si and Ti were determined by inductively coupled plasma emission spectrometry (ICP) on a Thermo IRIS Intrepid II XSP atomic emission spectrometer after dissolving the samples in HF solution. The textual properties of microporous/mesopores hybrid materials were analyzed by nitrogen adsorption–desorption at 77 K on a BELSORP-MAX instrument after degassing at 573 K under vacuum for 6 h. The surface area was calculated with the Brunauer-Emmett-Teller (BET) method, while the total pore volume was accumulated from the adsorption capacity at P/P_0 = 0.99. The micropore and mesopore size distributions were calculated by the Saito-Foley (SF) and Barrer-Joyner-Halenda (BJH) methods, respectively. The carbon content of the core-shell materials was detected by

thermogravimetric analysis (TG) in the temperature range of 303-1073 K under an air flow. Scanning electron microscopy (SEM) images were collected on a Hitachi S-4800 at 3 kV. The transmission electron microscopy (TEM) images were taken on a Tecnai G^2 F30 transmission electron microscope at 300 kV. Fourier transform infrared (FT-IR) spectra were collected on a Nicolet Nexus 670 FT-IR spectrometer operated at a spectral resolution of 2 cm^{-1} using KBr pellets of the solid samples. UV-visible (UV-vis) spectra were recorded on a Shimadzu UV-2700 spectrophotometer using $BaSO_4$ as a reference. Optical microscopy images were taken on an OLYMPUS TH4-200 light transmission microscope.

Emulsification formation

The emulsions, stabilized by the TS-1@Si/C composite in the 1-hexene/H_2O_2 system, were prepared following our previous report.[3] 50 mg TS-1@Si/C composite, 1.5 mL H_2O_2 (30 wt.%) aqueous solution and 1.5 mL 1-hexene were mixed at a water/oil volume ratio of 1:1. After homogenizing at 16000 rpm for 3 min with an ultraturax Fluko FA25 homogenizer equipped with a 10 mm dispersing tool, the mixture was kept static at ambient temperature for 60 min to estimate the stability of the emulsified phase.

Catalytic reactions

The catalytic performance of the TS-1@Si/C material under Pickering interfacial catalysis (PIC) and conventional catalytic condition were tested statically with 50 mg catalyst, 1.5 mL aqueous solution of H_2O_2 (30 wt.%) and 1.5 mL 1-hexene, that is, at a water/oil volume ratio of 1:1. The mixture was homogenized by a homogenizer at room temperature before the PIC tests, whereas the mixture was not homogenized under the conventional condition for control experiment. After the reaction at 333 K

for 1 h, the mixture was cooled to ambient temperature and centrifuged. The liquid products were analyzed by a Shimadzu GC-2014 gas chromatograph equipped with a FID detector and a HP5-MS capillary column (30 m × 0.25 mm × 0.25 μm).

The reusability of the TS-1@Si/C was evaluated in the epoxidation of 1-hexene with H_2O_2 under PIC condition. After each cycle, the catalyst was separated from the reaction system by centrifugation, washed using ethanol, and dried at 30 ºC.

Liquid-phase 1-hexene adsorption

The liquid-phase 1-hexene was performed by immersing 50 mg catalyst in mixture of 1.5 mL 1-hexene and 1.5 mL H_2O. The mixture was homogenized by a homogenizer at room temperature before adsorption tests. Then, the mixture was kept under static condition at 333 K for 1 h. The residual amount of 1-hexene was determined by a Shimadzu GC-2014 gas chromatograph equipped with a FID detector and a HP5-MS capillary column (30 m × 0.25 mm × 0.25 μm).

Table S1. Physicochemical properties of TS-1 and core-shell structured TS-1 samples.

No.	Sample	SSA[a] ($m^2 g^{-1}$)	S_{ext}[b] ($m^2 g^{-1}$)	V_{total}[c] ($cm^3 g^{-1}$)	V_{micro}[b] ($cm^3 g^{-1}$)	V_{meso}[d] ($cm^3 g^{-1}$)	D_{meso}[e] (nm)	Carbon content[f] (wt.%)
1	TS-1	406	20	0.28	0.21	0.07	-	-
2	TS-1@Si/C-3	487	91	0.31	0.19	0.12	2.46	12.6
3	TS-1@Si/C-7	502	105	0.46	0.20	0.26	2.46	7.5
4	TS-1@Si/C-13	507	113	0.52	0.20	0.32	2.46	4.9
5	TS-1@Si/C-19	518	122	0.59	0.22	0.37	2.46	2.9
6	TS-1@Si/C-30	523	157	0.61	0.21	0.40	2.46	1.3
7	TS-1@Si/C-50	539	169	0.65	0.20	0.45	2.46	0.9
8	TS-1@C-D	453	22	0.29	0.21	0.07	-	-
9	TS-1@Si-D	552	175	0.54	0.22	0.32	2.46	-

[a] Specific surface area (SSA) calculate by BET method

[b] Obtained by *t*-plot method.

[c] Pore volume measured at $P/P_0 = 0.99$.

[d] $V_{meso} = V_{tot} - V_{micro}$

[e] Calculated by BJH method.

[f] Determined by TG analysis from the weight loss in the temperature range of 303 - 1073 K.

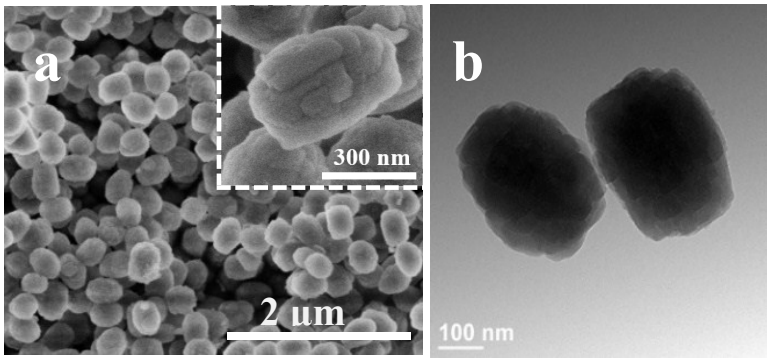

Figure S1 SEM and TEM micrographs of TS-1 (a and b)

The pristine TS-1 crystals were uniform nanosphere aggregation with an average particle size of 200 nm (Fig. S1, ESI).*

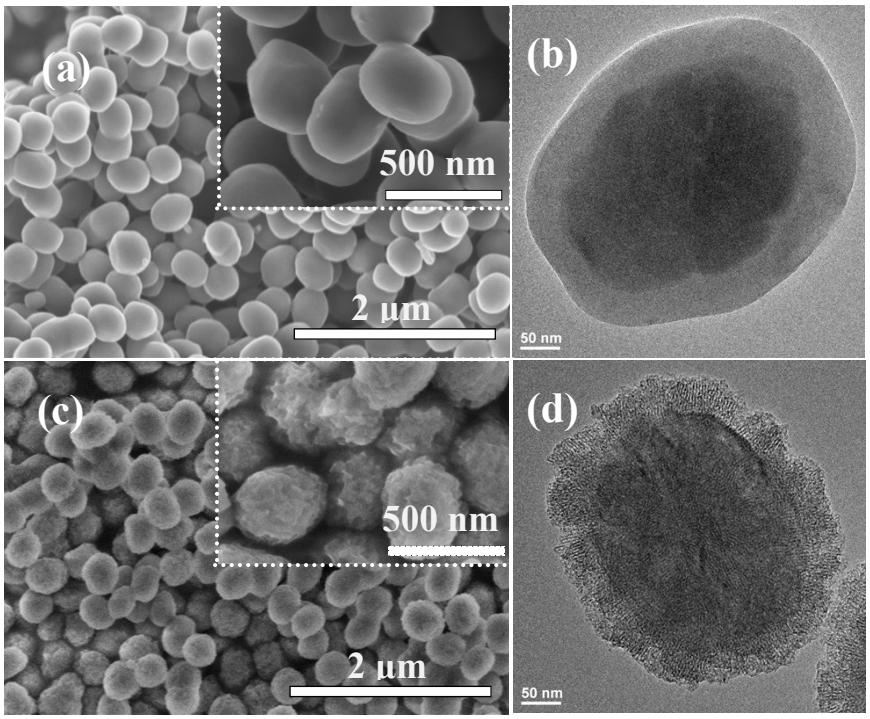

Figure S2 SEM and TEM micrographs of TS-1@C-D (a and b) and TS-1@Si-D (c and d).

Both TS-1@C-D and TS-1@Si-D materials could be synthesized to have uniform core-shell structure. TS-1@C-D showed a smooth surface, while TS-1@Si-D had a rough surface (Fig. S2a and S2c, ESI). In the TEM images, the dendritic pores of center-radial mesopore channels could be clearly observed for TS-1@Si-D material (Fig. S2d, ESI*), which was similar to that of TS-1@Si/C composite material. In contrast, no mesopore channels could be found in the shell of TS-1@C-D material (Fig. S2b, ESI*), indicating that the silicate species play an important part in controlling the surfactant-assisted assembly of mesopores in the shell.*

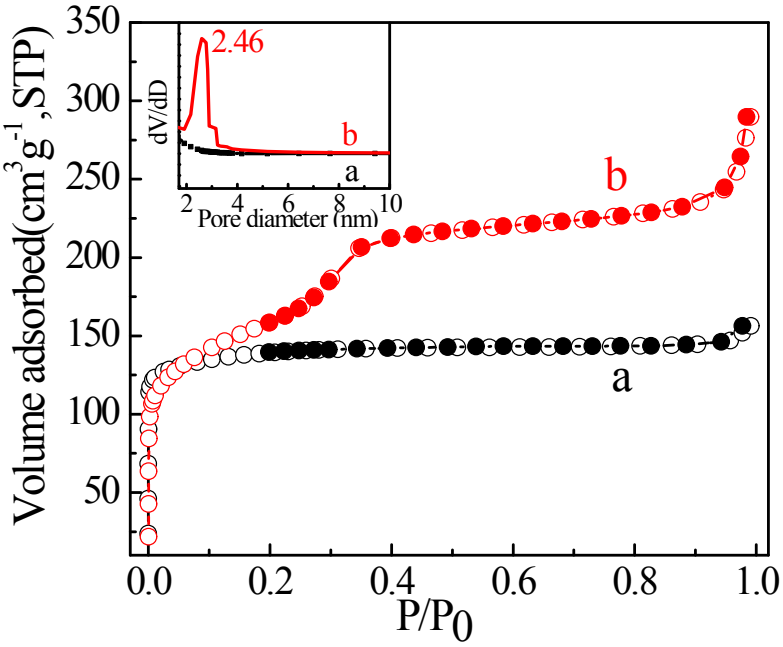

Figure S3 N_2 adsorption-desorption isotherms at 77 K of TS-1@C-D (a) and TS-1@Si-D (b). The inset shows corresponding pore diameter distribution for TS-1@C-D (a) and TS-1@Si-D (b).

TS-1@C-D material, with only carbon component in the shell, exhibited a type I sorption isotherm (Fig. S3a, ESI), while TS-1@Si-D material showed the sorption isotherms with the characterization of both type I and type IV (Fig. S3b, ESI*), indicative of both micropores and mesopores. The N_2 adsorption results were in good agreements with that from SEM and TEM images evidence in Fig. S2. The inset gave the mesopore distribution for TS-1@C-D and TS-1@Si-D materials. TS-1@Si-D showed a well-defined peak around 2.46 nm in the shell, while no peak was observed for TS-1@C-D material. The mesopores of TS-1@Si/C (2.46 nm, Fig. 1Bb) was comparable to that of TS-1@Si-D, indicating the carbon species almost had no influence on the pore size.*

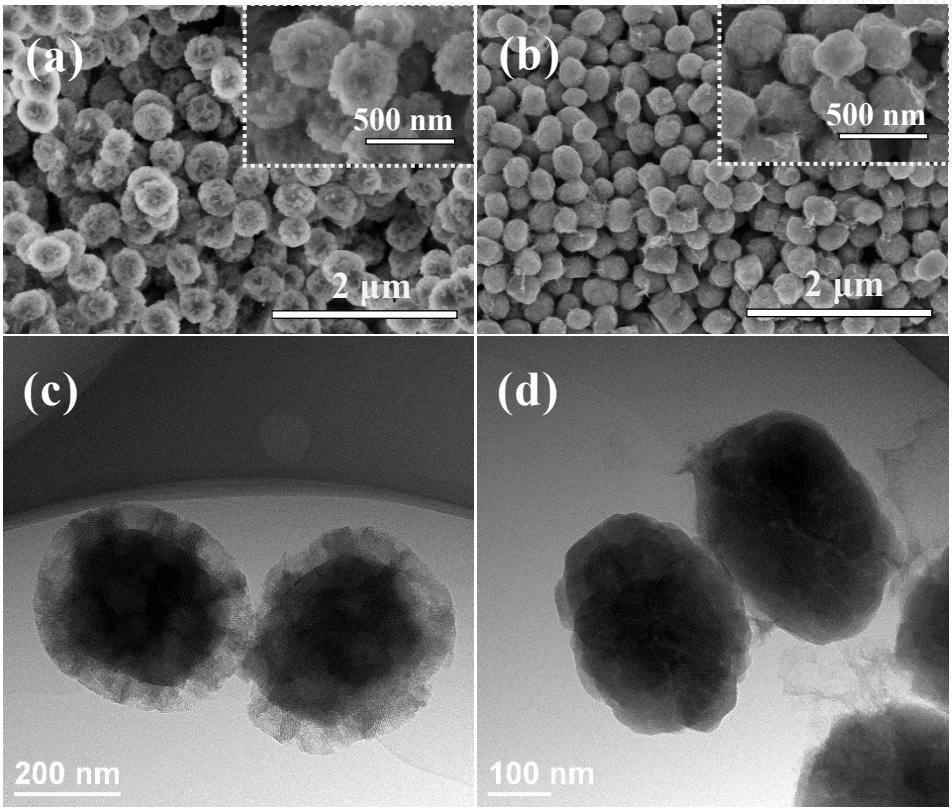

Figure S4 SEM and TEM micrographs of TS-1@Si-R (a and c) and TS-1@C-R (b and d).

After removing carbon from the shell, the TS-1@Si-R exhibited a core/shell structure (Fig. S4a and S4c, ESI), very similar to that of TS-1@Si/C material (Fig. 1C and 1D). TS-1@C-R was prepared via selectively etching the mesosilica shell without damaging the core. The core/shell structure was destroyed for TS-1@C-R material with some debris on the surface of TS-1 core, as shown by the SEM and TEM images (Fig. S4b and S4d, ESI*). The results obtained by selective extraction of silica or carbon component from the shell again proved that the silica component was responsible for mesoporosity.*

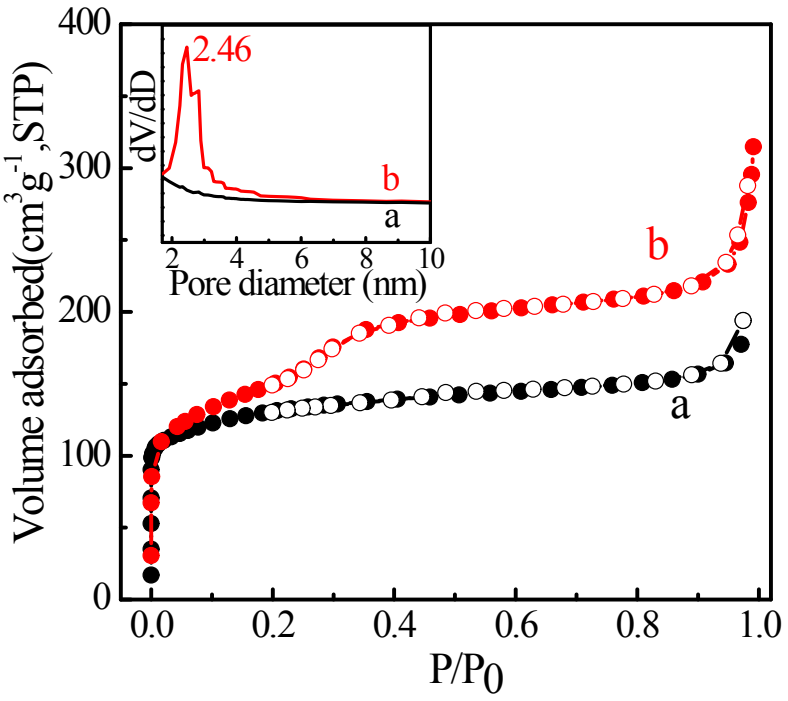

Figure S5 N_2 adsorption-desorption isotherms at 77 K of TS-1@C-R (a) and TS-1@Si-R (b). The inset shows corresponding pore diameter distributions for TS-1@C-R (a) and TS-1@Si-R (b).

After the removal of the amorphous silica from TS-1@Si/C by selective etching, the TS-1@C-R sample showed a type I adsorption isotherm (Figure S5a, ESI), indicating no mesopores structure in the shell. While selective burning carbon component in TS-1@Si/C, the TS-1@Si-R showed the isotherms combining type I and type IV characteristics (Figure S5b, ESI*), indicating the presence of both micropores and mesopores. The pore size distribution showed that the TS-1@Si-R sample possessed the mesopores with the size around 2.46 nm while no peak could be observed for TS-1@C-R. The N_2 adsorption results were in good agreement with that evidenced by the TEM and SEM images (Fig. S4, ESI*), indicating that the silica species is responsible for supporting the mesoporous shell structure.*

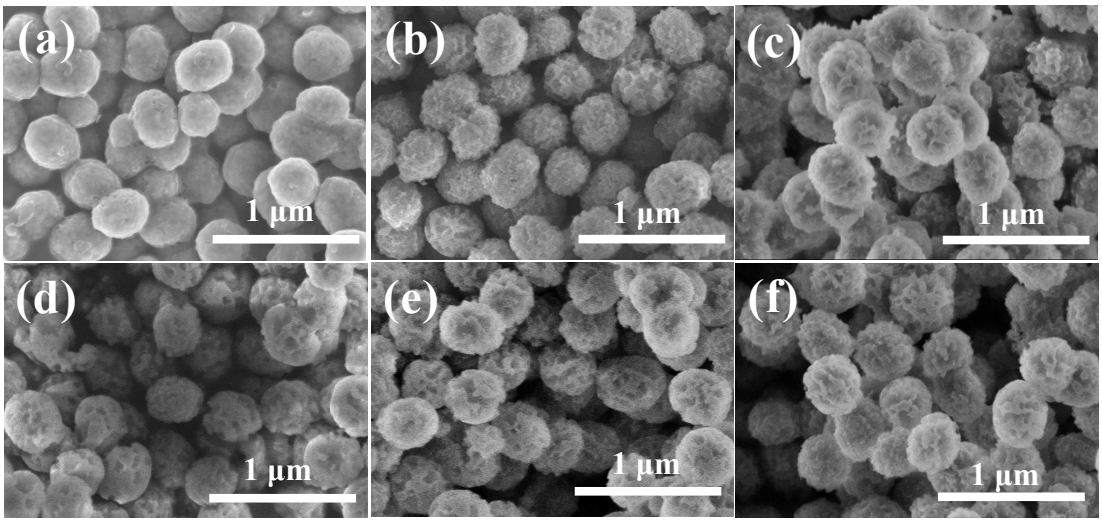

Figure S6 SEM micrographs of TS-1@Si/C-3 (a), TS-1@Si/C-7 (b), TS-1@Si/C-13 (c), TS-1@Si/C-19 (d), TS-1@Si/C-30 (e), TS-1@Si/C-50 (f).

The TS-1@Si/C-x (x=3-50) nanocomposites synthesized with different Si/C ratios all showed rough surface and uniformly dispersed spheres. Moreover, the surface roughness slightly changed among the samples, and higher TEOS/resorcinol (T/R) ratios resulted in a rougher surface (Fig. S6, ESI). All the nanospheres exhibited an increased particle size compared with the pristine TS-1 (Fig. S1a, ESI*), indicating that the core/shell materials have been successfully synthesized.*

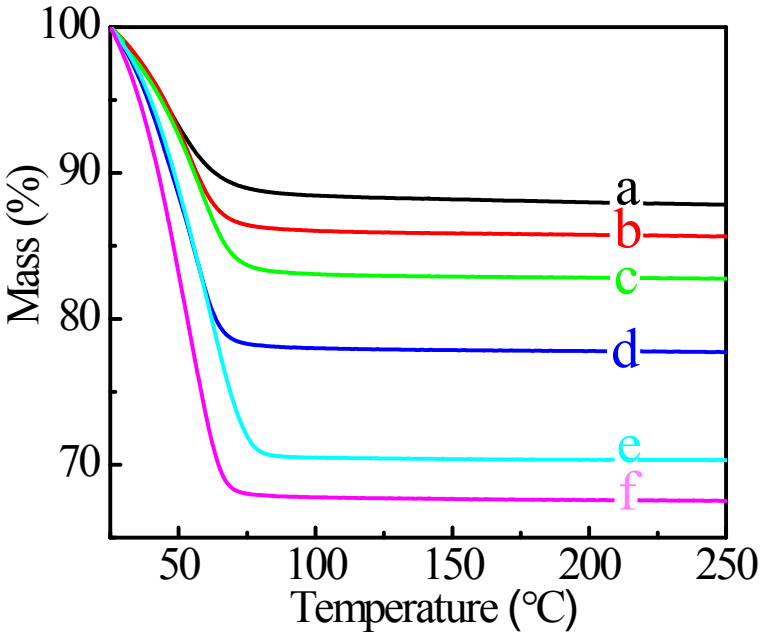

Figure S7 TG analyses of TS-1@Si/C-3 (a), TS-1@Si/C-7 (b), TS-1@Si/C-13 (c), TS-1@Si/C-19 (d), TS-1@Si/C-30 (e) and TS-1@Si/C-50 (f) after saturated with water vapor overnight in a desiccator.

TG analyses were performed to assess the hydrophilicity/hydrophobicity of all the composite materials with different Si/C ratios after saturated with water vapor overnight in a desiccator (Fig. S7, ESI). The weight loss in the temperature range of 30-200 ºC was mainly due to the physisorbed water, while that at higher temperatures was contributed by the decomposition of carbon species in shell part. The loss of water increased with increasing the T/R ratio from 3 to 50, indicative of enhanced hydrophilicity. Thus, the hydrophilicity/hydrophobicity of the TS-1@Si/C can be adjusted via varying the TEOS/resorcinol ratio in initial self-assembly process.*

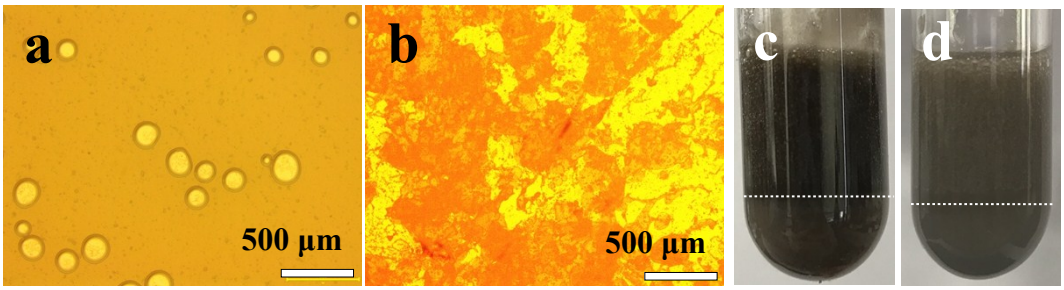

Figure S8 Optical microscopy image of 1-hexene/H_2O_2 Pickering emulsions stabilized by TS-1 (a) and TS-1@Si/C-3 (b). Appearance of 1-hexene/hydrogen peroxide (30 wt.%) system in the presence of TS-1@Si/C-30 (c) and TS-1@Si/C-50 (d) after homogenization and forming a Pickering emulsion.

Ideal particles suitable for Pickering emulsions should be nanosized and monodispersed, with regular morphology and with a suitable hydrophilic/hydrophobic balance (HLB). The optical microscopy image of 1-hexene/hydrogen peroxide system with TS-1 inside showed several air bubbles after homogenization, indicating that Pickering emulsion was failed to form due to hydrophilic characterization of TS-1 zeolite (Fig.S8a, ESI). The optical microscopy image shows that 1-hexene/H_2O_2 Pickering emulsion can be stabilized by TS-1@ Si/C-x (x=7-19) (Fig. 2d). In contrast, no droplets were observed for TS-1@Si/C-3 under the same condition (Fig.S8b, ESI*) due to the high content of hydrophobic carbon in the shell. Appearance of 1-hexene/hydrogen peroxide (30 wt.%) system in the presence of TS-1@Si/C-x (x=30, 50) showed phase separation after homogenization (Fig. S8c and S8d, ESI*) in virtue of the high hydrophilicity. These results showed that the TS-1@Si/C with appropriate silicon/carbon ratio in the shell, that is, suitable HLB property helped to stabilize the Pickering emulsion.*

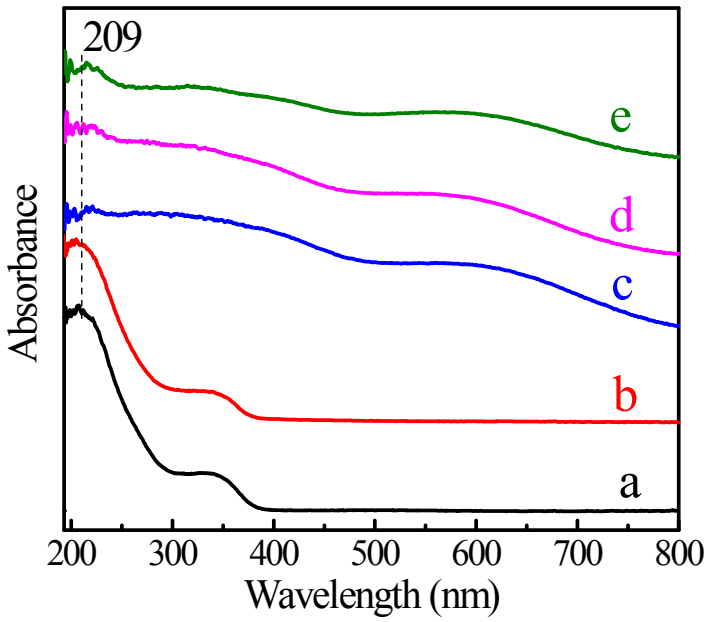

Figure S9 UV-vis spectra of TS-1 (a), TS-1@Si-D (b), TS-1@Si/C-7 (c), TS-1@Si/C-13 (d) and TS-1@Si/C-19 (e).

The pristine TS-1 showed a main adsorption band at 209 nm due to the tetrahedral Ti ions in the framework, together with a weak one at 330 nm contributed by anatase-like extra framework Ti species (Fig. S9a, ESI). After fabricating the mesostructured silica and carbon on the TS-1 crystal surface, a broad adsorption appeared in a wide visible region of 500-770 nm, due to the presence of carbon in the shell. In contrast, no such band was observed for the sample TS-1@Si-D with only silica component in the shell (Fig. S9b, ESI*). On the other hand, the characteristic adsorption of the tetrahedral Ti species was still observed at 209 nm in the TS-1@Si/C materials (Fig. S9c, 9d and 9e, ESI*), meaning the coating of Si/C didn't alter the coordination state of Ti species in TS-1 zeolite core. The intensity of both bands for TS-1@Si/C materials was lower than that of TS-1 due to the dilution effect.*

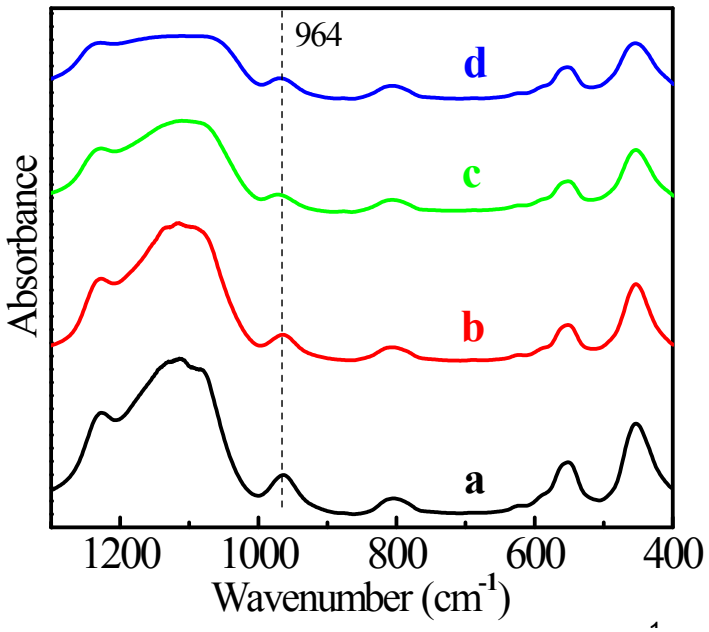

Figure S10 IR spectra of TS-1 (a), TS-1@Si/C-7 (b), TS-1@Si/C-13 (c) and TS-1@Si/C-19 (d).

Both TS-1 and TS-1@Si/C possessed the vibration band at 964 cm^{-1} (Fig. S10, ESI), which is a proof for the existence of framework Ti^{4+} in zeolite. In agreement with the former observation on the UV-vis spectra (Fig. S9, ESI*), the intensity of the 964 cm^{-1} band is lower for TS-1@Si/C materials than that for TS-1.*

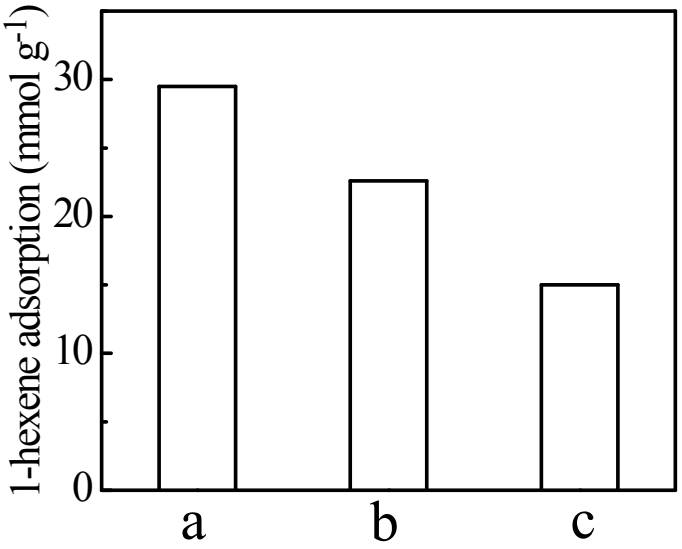

Figure S11 Uptake of 1-hexene in liquid-phase adsorption under PIC condition. TS-1@Si/C-7 (a), TS-1@Si/C-13 (b) and TS-1@Si/C-19 (c). Adsorption condition: cat., 50 mg; 1-hexene, 12.1 mmol (1.5 mL); H_2O, 83.3 mmol (1.5 mL); temp., 333 K; time 1 h; static condition.

The adsorption ability of 1-hexene molecules on the TS-1@Si/C decreased with the increase of the T/R ratio from 7 to 19 (Fig. S11, ESI). The higher carbon content in shell enhanced the hydrophobicity of TS-1@Si/C, which favored the adsorption of organic substrate 1-hexene.*

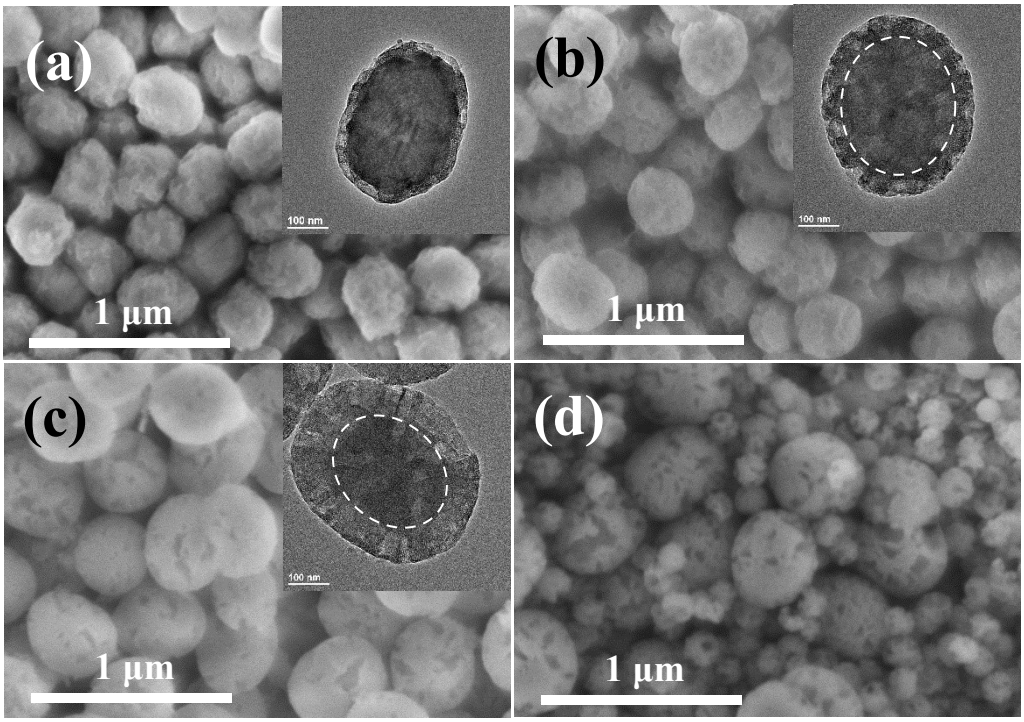

Figure S12 SEM and TEM micrographs of TS-1(0.2)@Si/C-13 (a), TS-1(0.5)@Si/C-13 (b), TS-1(1.2)@Si/C-13 (c) and TS-1(2.0)@Si/C-13 (d).

The SEM images of TS-1(0.2)@Si/C-13, TS-1(0.5)@Si/C-13 and TS-1(1.2)@Si/C-13 nanocomposites synthesized with the same T/R ratio all showed uniformly dispersed spheres (Fig. S12a, S12b and S12c, ESI). Nevertheless, the TS-1(2.0)@Si/C-13 showed phase separation due to the low content of TS-1 in the synthetic system (Fig. S12d, ESI*). The TEM showed that the shell thickness increased from 10 to 120 with the decreasing of TS-1 content from 1.2 to 0.2 g in the synthesis system (Fig. S12a, S12b, 2Dand S12c, ESI*).*

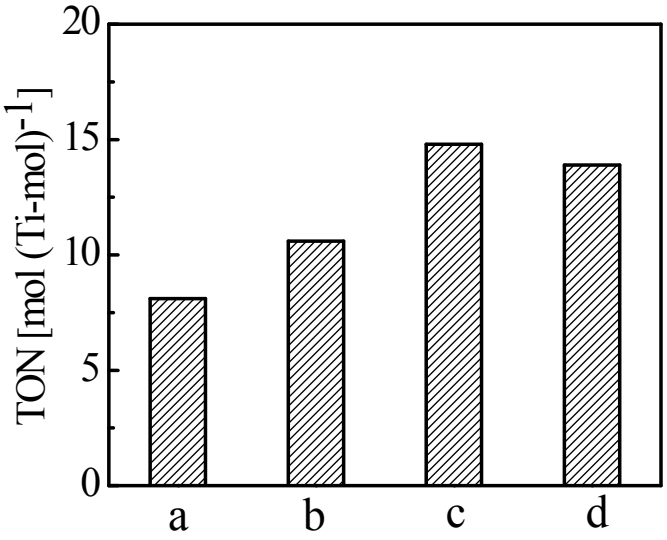

Figure S13 TON value of TS-1(0.2)@Si/C-13 (a), TS-1(0.5)@Si/C-13 (b), TS-1@Si/C-13 (c) and TS-1(1.2)@Si/C-13 (d) catalysts in the epoxidation of 1-hexene under the conditions of Pickering interfacial catalysis (PIC). Reaction conditions: cat., 50 mg; 1-hexene, 12.1 mmol; H_2O_2 (30 wt.%), 15.0 mmol; temp., 333 K; time, 1 h; static condition.

Compared with the TS-1(0.2)@Si/C-13, TS-1(0.5)@Si/C-13 and TS-1(1.2)@Si/C-13, the TS-1@Si/C-13 catalyst with suitable shell thickness showed higher activity. On one hand, the adsorption of water and 1-hexene on TS-1@Si/C was increased with the increase of shell thickness (Fig. S14 and S15, ESI), favoring the catalytic performance under PIC condition. On the other hand, the thicker shell would increase the diffusion path of 1-hexene to the Ti peroxo species generated on the encapsulated TS-1. Considering the two factors, the TS-1@Si/C-13 catalyst exhibited a higher activity than TS-1 (0.2)@Si/C-13, TS-1 (0.5)@Si/C-13 and TS-1 (1.2)@Si/C-13.*

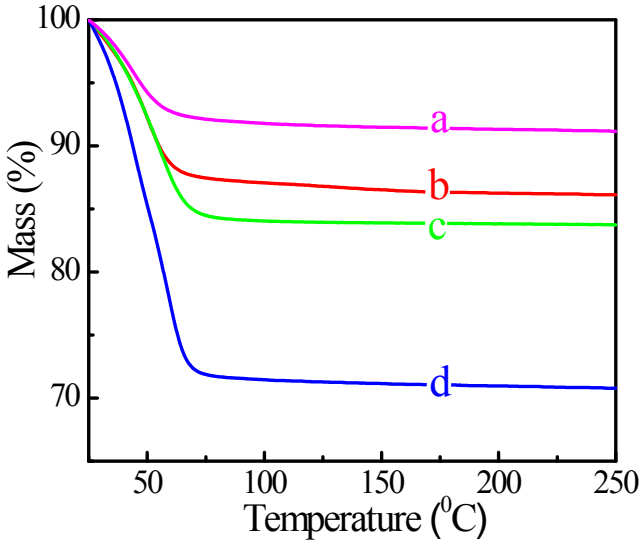

Figure S14 TG analyses of TS-1(0.2)@Si/C-13 (a), TS-1(0.5)@Si/C-13 (b), TS-1@Si/C-13 (c) and TS-1 (1.2)@Si/C-13 (d) after saturated with water vapor overnight in a desiccator.

The loss of water increased with increasing the shell thickness, meaning that the thicker shell helped to increase the absorption ability of aqueous H_2O_2, due to higher hydrophilic silica content of TS-1@Si/C.

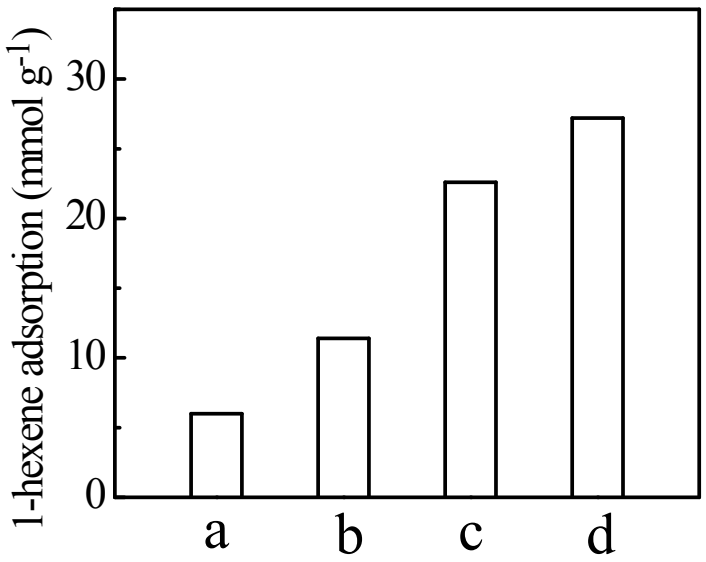

Figure S15 Uptake of 1-hexene in liquid-phase adsorption under PIC condition. TS-1(0.2)@Si/C-13 (a), TS-1(0.5)@Si/C-13 (b), TS-1@Si/C-13 (c) and TS-1(1.2)@Si/C-13 (d). Adsorption condition: cat., 50 mg; 1-hexene, 12.1 mmol (1.5 mL); H_2O, 83.3 mmol (1.5 mL); temp., 333 K; time 1 h; static condition.

With the increase of shell thickness, the adsorption of 1-hexene molecules on TS-1@Si/C was increased due to increased carbon content in the TS-1@Si/C, favoring the catalytic performance under PIC condition (Fig. S15, ESI).*

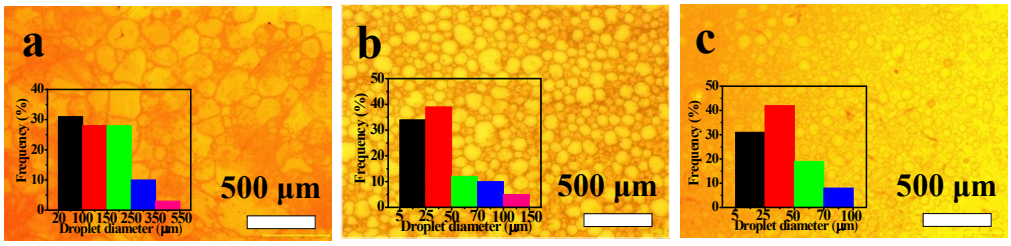

Figure S16 Optical microscopy image of a 1-hexene/H_2O_2 (30 wt.%) Pickering emulsion stabilized by TS-1@Si/C-13 with the catalyst amount of 30 mg (a), 50 mg (b) and 70 mg (c).

To obtain the different droplet sizes, different amount of TS-1@Si/C-13 catalysts have been added to the Pickering emulsion system. As displayed in Fig. S16, the average droplet diameter decreased from 127 to 45 and 39 μm with the amount of TS-1@Si/C-13 increased from 30 to 50 and 70 mg.

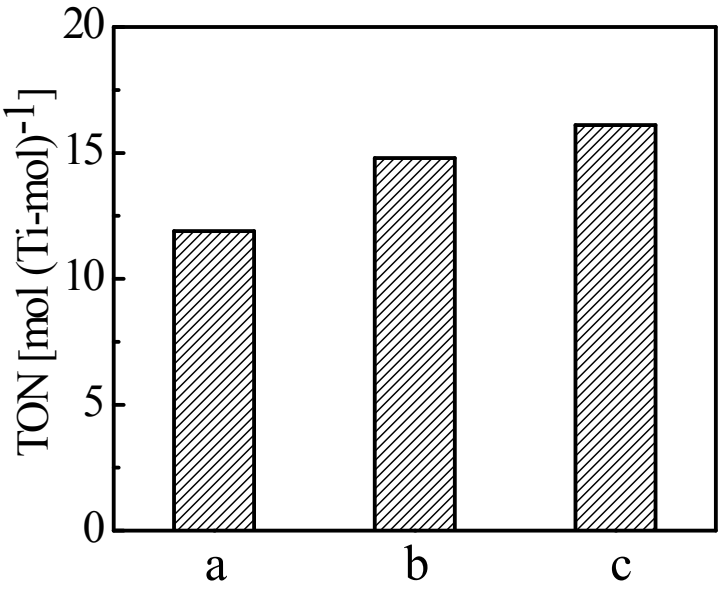

Figure S17 TON value of TS-1@Si/C-13 with the catalyst amount of 30 mg (a), 50 mg (b) and 70 mg (c) in the epoxidation of 1-hexene under the conditions of Pickering interfacial catalysis (PIC). Reaction conditions: 1-hexene, 12.1 mmol; H_2O_2 (30 wt.%), 15.0 mmol; temp., 333 K; time, 1 h; static condition.

With the increase of the amount of TS-1@Si/C-13, the activity was increased with the decrease of droplet size, due to shorter diffusion distance (Fig. S17, ESI).*

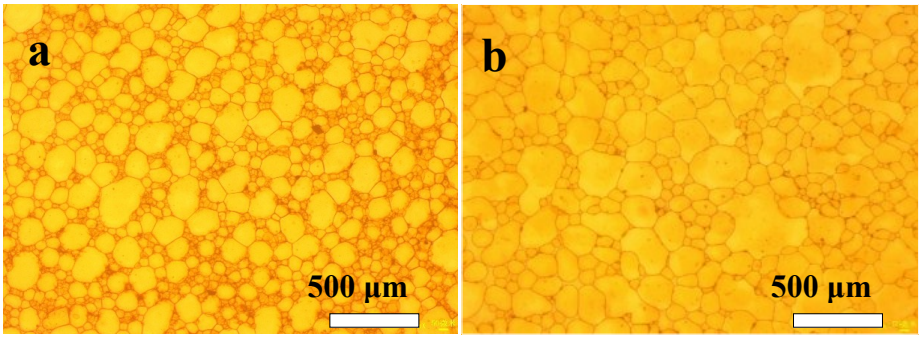

Figure S18 Optical microscopy image of a 1-hexene/H_2O_2 (30 wt.%) Pickering emulsion stabilized by TS-1@Si/C-13 after standing for 48 h (a) and catalytic reaction (b).

The Pickering emulsion remained stable even after deposited at room temperature for 48 h (Fig. S18a, ESI) or under reaction condition (Fig. S18b, ESI*) with the droplets becoming bigger, showing good stability.*

References

1. M. Taramasso, G. Perego and B. Notari, *US Patent*, 1983, 4410501.
2. H.G. Peng, X. H. Li, L. Xu, P. Wu, *Chin. Chem. Lett.*, 2013, **24**, 559.
3. Y. Yang, W. Zhou, A. Liebens, J. Clacens, M. Pera-Titus, P. Wu, *J. Phys. Chem. C,* 2015, **119,** 25377.